Available online at www.sciencedirect.com
ScienceDirect
International Journal of Mass Spectrometry 265 (2007) 30–39
International Journal of Mass Spectrometry
www.elsevier.com/locate/ijms

Development and characterization of an ion trap mass spectrometer for the on-line chemical analysis of atmospheric aerosol particles

Andreas Kürten [a], Joachim Curtius [b,*], Frank Helleis [a], Edward R. Lovejoy [c], Stephan Borrmann [a,b]

[a] *Max Planck Institute for Chemistry, Particle Chemistry Department, Mainz, Germany*
[b] *Johannes Gutenberg University, Institute for Atmospheric Physics, J.J. Becherweg 21, D-55128 Mainz, Germany*
[c] *National Oceanic and Atmospheric Administration, Earth System Research Laboratory, Chemical Sciences Division, Boulder, USA*

Received 26 January 2007; received in revised form 9 May 2007; accepted 16 May 2007
Available online 21 May 2007

Abstract

A novel Ion Trap Aerosol Mass Spectrometer (IT-AMS) for atmospheric particles has been developed and characterized. With this instrument the chemical composition of the non-refractory component of aerosol particles can be measured quantitatively. The set-up makes use of the well-characterized inlet and vaporization/ionization system of the Aerodyne Aerosol Mass Spectrometer (AMS). While the AMS uses either a linear quadrupole mass filter (Q-AMS) or a time-of-flight mass spectrometer (ToF-AMS) as the mass analyzer, the IT-AMS utilizes a three-dimensional quadrupole ion trap. The main advantages of an ion trap are the possibility of performing MS^n-experiments as well as ion/molecule reaction studies. The mass analyzer has been built in-house together with major components of the electronics. The IT-AMS is operated under full PC control and can be used as a field instrument due to its compact size. A detailed description of the set-up is presented. Experiments show that a mass resolving power larger than 1500 can be reached. This value is high enough to separate different organic species at *m/z* 43. Calibrations with laboratory-generated aerosol particles indicate a linear relationship between signal response and aerosol mass concentration. These studies, together with estimates of the detection limits for particulate sulfate (0.65 $\mu g/m^3$) and nitrate (0.16 $\mu g/m^3$) demonstrate the suitability of the IT-AMS to measure atmospheric aerosol particles. An inter-comparison between the IT-AMS and a Q-AMS for nitrate in urban air yields good agreement. For laboratory-generated polystyrene latex particles a MS/MS-study using collision-induced dissociation (CID) with a daughter/parent ion yield of more than 60% has been performed. In the future, similar MS/MS-studies can be conducted for atmospheric particles and for the study of secondary aerosol formation in smog chamber experiments.

Keywords: Ion trap; Modified angle trap; Mass spectrometry; Aerosol mass spectrometer; AMS

1. Introduction

The chemical analysis of aerosol particles with on-line mass spectrometric methods is of interest in many scientific fields. The contributions of these methods for understanding atmospheric chemistry and climate have recently been reviewed [1]. However, many open questions remain. Especially the processes that lead to the formation of secondary organic aerosol (SOA) components are widely unknown. This is mainly due to the huge variety and complexity of organic compounds found in the atmosphere [2]. In addition, analysis of these compounds is complicated by their fragility [3]. Therefore, the development of new sensitive mass spectrometric methods with soft ionization techniques can help to identify such components in atmospheric particles.

Aerosol mass spectrometry has been the topic of several recent review articles [4–6]. Many existing aerosol mass spectrometers either use time-of-flight mass spectrometers or linear quadrupole mass filters. Nevertheless, in several studies an ion trap has been used for the chemical analysis of aerosol particles. Especially the Laser Spectroscopy and Chemical Microtechnology Group at Oak Ridge National Laboratory has pioneered the application of ion trap mass spectrometry for the on-line analysis of aerosol particles [7–12]. Some advantages of ion trap mass spectrometry are: (1) the compactness of the mass analyzer, (2) a high duty-cycle (fraction of the time spent for ion

* Corresponding author.
E-mail address: curtius@uni-mainz.de (J. Curtius).

1387-3806/$ – see front matter © 2007 Elsevier B.V. All rights reserved.
doi:10.1016/j.ijms.2007.05.007

accumulation to the total measuring time) can be achieved, (3) a complete mass spectrum can be recorded for individual particles, (4) reactions inside the trap can be studied, (5) a large mass range is accessible and (6) MS^n-studies can be performed.

Contributions to the field of aerosol ion trap mass spectrometry can be categorized according to the method of particle vaporization and the subsequent ionization processes. Laser desorption/ionization can be used for single particles in the center of an ion trap by firing an intense laser pulse through a hole in one of the electrodes. The trigger for the laser pulse is determined by the particle velocity which is measured by scattered light signals from two continuous lasers in front of the trap. This method has been used, e.g., to study single bacteria [7], polycyclic aromatic hydrocarbons (PAHs) in particles from diesel engine exhaust [8] or uranium and uranium oxides in airborne particles [9]. In these studies an inlet system consisting of a nozzle and two skimmers was used, recent modifications of the instrument operate with an aerodynamic lens [10,11]. Using an aerodynamic lens and an optimized detection system, single particles with diameters as small as ~200 nm can be analyzed with high efficiency by a portable instrument. However, quantitative measurements are limited when using the laser ablation technique.

An instrument that also analyzes single particles by laser ablation is the nanoaerosol mass spectrometer (NAMS) that is used for particles with sizes of ~10 nm [13,14]. Since it is not possible to detect these particles by their scattered light, charged particles are captured in the trap. A high-energy laser pulse (150 mJ) that is focused tightly (fluence ~100 J/cm^2) creates a plasma, therefore only atomic fragment ions are produced. These ions are ejected from the trap and analyzed in a reflectron/time-of-flight mass spectrometer.

Hoffmann et al. [15] describe an instrument that has mainly been used for the analysis of secondary organic aerosol particles. The particles are vaporized inside a heated tube, ionized at atmospheric pressure by chemical ionization (APCI) and are subsequently analyzed in an ion trap. A similar method has been used by Dalton et al. [16] by combining glow discharge ionization (GDI) with ion trap mass spectrometry.

Harris et al. [12] have very recently reported the application of a modified commercial ion trap for the study of warfare-related species on aerosol particles. The particles are brought into the vacuum by an aerodynamic lens and are thermally vaporized inside the ion source region. Ions are created externally either by electron impact or chemical ionization.

Here we present a novel Ion Trap Aerosol Mass Spectrometer (IT-AMS). The IT-AMS provides on-line measurements of the chemical composition of the non-refractory component of aerosol particles. The three-dimensional quadrupole ion trap mass analyzer has been designed and machined in-house. It is combined with an inlet and evaporation/ionization system taken from the commercial Aerosol Mass Spectrometer (AMS, Aerodyne Research Inc., USA) that contains an aerodynamic lens, a vaporizer and an electron impact (EI) ion source.

In this paper we describe the set-up of the IT-AMS. Results from characterization studies are shown that include a mass calibration measurement, a comparison with a Quadrupole-AMS (Q-AMS) for urban particulate nitrate and a MS/MS-experiment for laboratory-generated polystyrene latex particles.

2. Experimental set-up and theory of operation

The Ion Trap Aerosol Mass Spectrometer is a combination of a three-dimensional quadrupole ion trap mass spectrometer and an aerosol inlet chamber containing an evaporation/ionization system. The latter one has been purchased from Aerodyne (Aerodyne Inc., USA) and is identical to the system used by the commercial Aerosol Mass Spectrometer. The AMS uses either a linear quadrupole mass filter (Q-AMS [17]) or a time-of-flight mass spectrometer (ToF-AMS [18,19]) as the mass analyzer.

Fig. 1 shows a schematic diagram of the IT-AMS. The flow into the instrument is controlled by a critical orifice ($d \sim 120\,\mu m$) that maintains a flow rate of ~120 cm^3/min at ambient pressure and temperature. The aerosol passes through an aerodynamic lens that focuses the particles into a narrow beam [20,21]. At the same time the incoming gas is efficiently removed. The combination of these two effects results in a substantial enrichment of the particulate phase over the gas phase. The size range of particles that are transmitted by the aerodynamic lens with almost 100% efficiency is approximately 60–600 nm. The chopper wheel that is used within the AMS to provide size resolved chemical information about the particles [17] is currently not used for the IT-AMS because it is not possible to obtain size-resolved chemical information when using only one chopper wheel. This is due to the fact that the time needed to analyze ions within the IT-AMS is considerably longer than the difference in particle flight times due to their different sizes. Therefore, at the moment, only the integral chemical composition of all particle sizes is measured. Size resolved mass spectra could be obtained in the future by using two chopper wheels that are operated in a way that only a certain particle size range reaches the ion source and the trap.

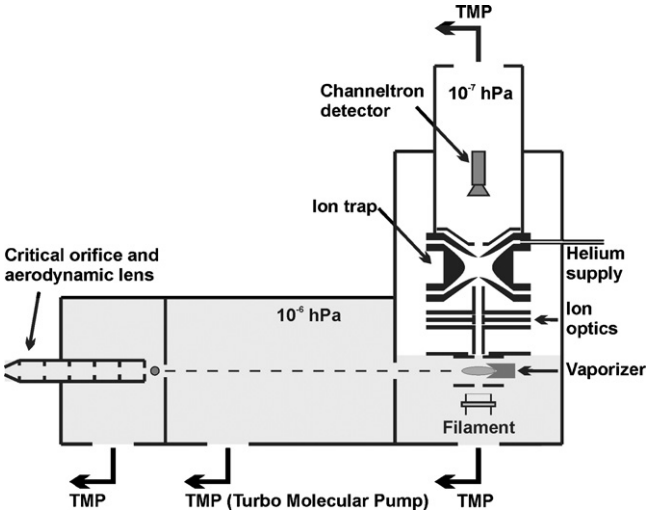

Fig. 1. Schematic diagram of the Aerosol Ion Trap Mass Spectrometer (IT-AMS). The IT-AMS is a combination of a flight chamber taken from the commercial Aerosol Mass Spectrometer (AMS, Aerodyne Research Inc., USA) shown with a gray background and a newly set-up three-dimensional quadrupole ion trap.

The aerosol particles traverse a flight chamber (~45 cm), impact on a resistively heated cartridge and are flash-vaporized. The vaporizer is cylindrically shaped (3.8 mm in diameter) and consists of porous tungsten. Both the material and the shape of the vaporizer are supposed to minimize losses due to particle bounce [22]. The standard Aerodyne vaporizer is used and no attempts were made to minimize particle bounce. The temperature is measured at the tip of the vaporizer by a thermocouple and is usually adjusted to ~600 °C. A more detailed description of the vaporizer and the flight chamber is given, e.g., by Drewnick et al. [18]. The vaporizer is placed inside an electron impact ion source where the particle vapor is ionized at 70 eV. Positive ions are accelerated out of the ion source and focused into the ion trap by several electrostatic lenses.

The ion trap consists of three electrodes, one ring electrode and two end cap electrodes with hyperboloidal shape and cylindrical symmetry around the z-axis (see Fig. 2). The curvature of the electrodes has a modified angle geometry [23] with $r_0 = 1$ cm and $z_0 = r_0/\sqrt{1.9} = 0.725$ cm. The parameters r_0 and z_0 determine the shortest distances from the center of the trap to the ring electrode and to the end cap electrodes. The geometry of the trap is identical with the one used by Curtius et al. [24]. Ions enter and leave the trap through an orifice (1.5 mm in diameter) in the front and rear end cap electrode, respectively. Ions are detected by use of an in-axis mounted channel electron multiplier operating in pulse counting mode.

Ultrapure helium is used as a buffer gas to increase trapping efficiency and mass resolution [25]. The helium is injected directly into the trap. A ceramic ring serves as a spacer between the ring electrode and the end cap electrode. It was found that sensitivity is best when only one ring is used that fully covers the space between the electrodes. Ceramic washers are used between the ring and the second end cap electrode. Helium buffer gas pressure is measured outside the ion trap and is usually adjusted to a pressure of 1×10^{-4} hPa (corrected for helium). This pressure was found to be a good compromise between signal intensity (which is higher for higher pressures) and mass resolving power (which is best for the chosen pressure). So far, it has not been tested in detail whether detection limits can be improved substantially when a higher buffer gas pressure is used and trapping efficiency is maximized. This strategy might be useful in cases when a low mass resolving power is tolerable and higher sensitivity is required.

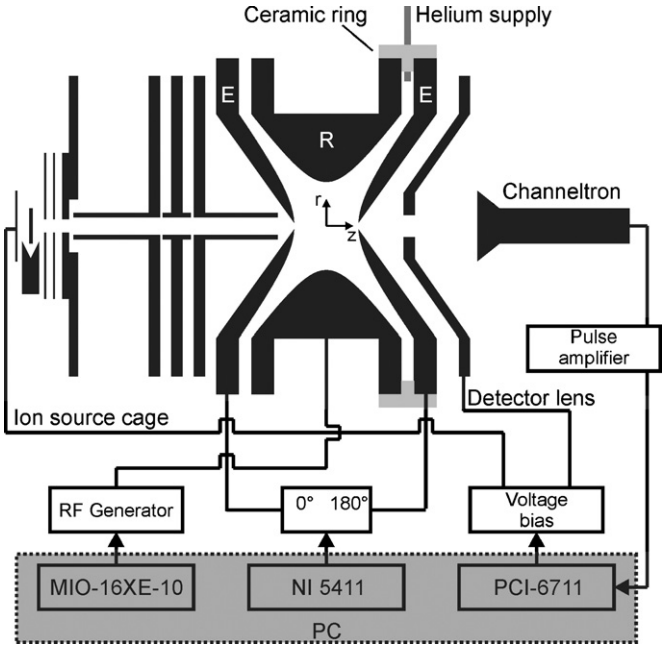

Fig. 2. Schematic diagram of the ion source, ion optics, ion trap, detector and the most important electronic components. The electronics are controlled by three National Instruments PCI boards in a PC. The boards control the RF voltage at the ring electrode R (MIO-16XE-10), the RF voltage waveforms at the end cap electrodes E (NI 5411) and a voltage bias for gating the voltages applied to the ion source cage and to the detector lens (PCI-6711). The PCI-6711 is also used for counting the ion pulses from a channel electron multiplier after amplification.

Electrode arrangement and voltage settings have been optimized using the Simion 7.0 ion trajectory simulation program [26]. Detailed simulation studies about the focusing of ions with this set-up and the numerical calculation of trapping efficiencies for different ion masses will be discussed in a forthcoming paper.

The trap is operated by applying a time-dependent voltage $U + V\cos(\Omega t)$ to the ring electrode, where U is the dc component and V is the ac component with the angular frequency Ω. From comparison of the equation of motion for ions inside the trapping field and the Mathieu equation two dimensionless stability parameters can be obtained for the z-direction [27]:

$$a_z = \frac{-16zeU}{m(r_0^2 + 2z_0^2)\Omega^2} \quad (1)$$

$$q_z = \frac{8zeV}{m(r_0^2 + 2z_0^2)\Omega^2} \quad (2)$$

where m is the ion mass and z is the number of elementary charges e. The values of the stability parameters determine if the ion motion is stable in the z-direction. The IT-AMS is operated with a zero dc component ($U = 0$), therefore only q_z is of interest. Since the values of r_0, z_0, Ω and m/z are constant for a given ion, only the magnitude of V determines whether ions remain inside the trap or not. When the end cap electrodes are grounded, ion trajectories become unstable at a q_z value of 0.908. By applying a supplementary ac voltage at the end cap electrodes, ions can also be ejected at lower q_z values, thereby expanding the maximum accessible mass range (see, e.g., ref. [28]). The frequency that must be applied to achieve ejection at a selected q_{eject} can be calculated by equations given by March [27]. The relation between the selected q_{eject}, the applied voltage V and the m/z that will become unstable under these conditions is:

$$\frac{m}{z} = \frac{8eV}{q_{\text{eject}}(r_0^2 + 2z_0^2)\Omega^2}. \quad (3)$$

The ion trap is controlled by a PC equipped with three National Instruments PCI boards (National Instruments, USA). These boards are a PCI-MIO-16XE-10 and a PCI-6711 multifunction data acquisition card and a NI 5411 arbitrary waveform generator board. Fig. 2 shows schematically the ion source, the ion optics, the ion trap and the channeltron detector together with the most important components of the electronics.

The PCI-MIO-16XE-10 board is used for control of the RF voltage amplitude. The voltage at the ring electrode is supplied by an RF voltage supply (QMH 410-2, Pfeiffer Vacuum GmbH, Germany) with a fixed frequency ($f = \Omega/(2\pi) = 1.3$ MHz) and a maximum voltage of 3.13 kV (zero to peak). Therefore, the maximum accessible m/z value with grounded end-cap electrodes ($q_{eject} = 0.908$) can be calculated for the given dimensions to be ~200. This mass range can be extended by applying a supplementary sine wave at the end cap electrodes for resonant ejection as mentioned above [28]. We have demonstrated resonant ejection at as low as $q_z = 0.176$ thereby extending the mass range to more than 1000 amu.

The voltage waveforms for resonant excitation are created by the NI 5411. They are used for three purposes: (1) ejection of unwanted ions during ion accumulation to reduce space charge effects or to isolate ions for MS/MS, (2) to realize a mass range extension during ion ejection and (3) to stimulate collision induced dissociation (CID) of ions for MS/MS-studies. To realize (2) and (3) constant frequencies are used. For the ejection of unwanted ions (1) it is necessary to excite a range of m/z values. This is not possible with a single frequency. Instead voltage waveforms must be calculated by inverse Fourier transform that include the appropriate frequencies in the time-domain (Filtered Noise Fields, FNF or Stored Waveform Inverse Fourier Transform, SWIFT) as demonstrated in several studies (e.g., refs. [29,30]).

The third PCI board (PCI-6711) fulfills two functions. First, it is used to count ion signals from the channel electron multiplier (KBL 510, Dr. Sjuts Optotechnik GmbH, Germany) after these have been passed through a pulse discriminator and preamplifier (WMT PAD06, WMT-Elektronik GmbH, Germany). Second, it produces a signal to trigger two bias voltages. These voltages are applied to the ion source cage and to an electrostatic lens in front of the channeltron detector to gate the ion current from the ion source to the ion trap and from the ion trap to the detector, respectively. Fig. 3 shows the timing sequence for trapping ions and recording a mass spectrum. A cycle can be subdivided into four different intervals. The timing is controlled by the RF voltage amplitude at the ring electrode. Initially this voltage is zero and the trap is emptied from ions potentially remaining from a previous scan. Then the amplitude is switched to a non-zero value for a certain time to accumulate ions. An additional period can be selected in which new ions are not allowed to enter the trap. This phase can be used to study, for example, ion cluster dissociations or ion–molecule reactions in the trap. For analysis of the stored ions the RF amplitude is then ramped and the ions are ejected mass selectively. Additional waveforms can be applied to the end cap electrodes for ejection of unwanted ions during ion accumulation or for application of waveforms to perform mass range extension during the ramping of the voltage. It is crucial that during that time no new ions enter the trap because the majority of these ions would simply fly through the trap and reach the detector. This is due to the relatively low trapping efficiency of approximately 1–5% for externally generated ions (also see below). Therefore, some portion of the ions that are not trapped would arrive randomly at the detector and the signals would overlap with signals from stored ions, thereby strongly

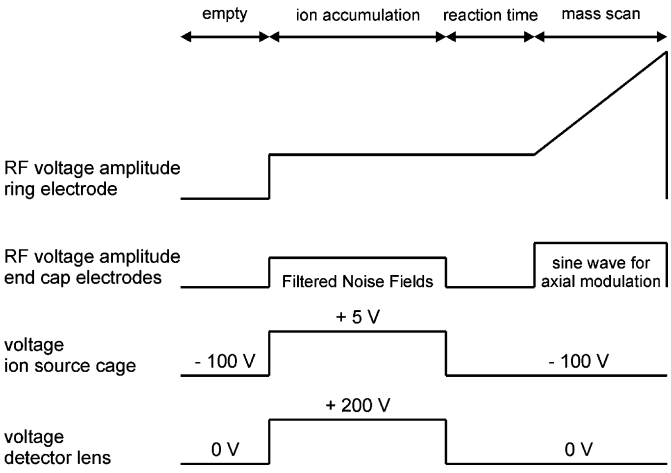

Fig. 3. The timing sequence (scan function) for the operation of the IT-AMS. Each cycle can be divided into four different intervals. First, the trap is emptied from ions of a previous scan, then ions are accumulated in the second period. A reaction time between ion accumulation and the mass scan is optional. For the mass scan the peak amplitude of the RF voltage is ramped. Only during the ion accumulation phase ions are allowed to enter the trap by applying a gate voltage to the ion source cage. In this time period a second gating voltage is applied to the detector lens to protect the channeltron. Operations such as ejection of unwanted ions and mass range extension are realized by voltage waveforms applied to the end cap electrodes. MS/MS-experiments are realized by an additional period between the reaction time and the mass scan (not shown).

reducing the signal-to-noise ratio. Several designs were tried in order to shut off the ion current efficiently and it was found that gating of the ion source cage gives the best results. Usually 5 V are applied to the cage of the cross-beam ion source and −65 V to the filaments (all voltages are referenced to the dc potential at the ring electrode). The emitted electrons are thereby accelerated to 70 eV into the cage where ions are formed. To shut off the ion current the voltage at the cage is switched to −100 V which does not allow the electrons to enter the cage anymore. Switching the filament voltage is not sufficient because the vaporizer which is located inside the cage emits ions itself. These ions are created by impurities in the vaporizer material containing sodium and potassium which are efficiently surface ionized at the operating temperatures (~600 °C) of the vaporizer. Gating the cage voltage to −100 V also prevents these ions from reaching the trap which would not be possible when gating the filament voltages. Other try-outs for shutting off the ion current included gating the voltage of one of the electrostatic lenses to high positive voltages or gating all the electrode voltages in front of the trap to negative values. However, in these experiments the desired efficiency was not reached. A similar procedure is used to protect the channeltron from ions during ion accumulation. As mentioned above, a substantial fraction of ions that reach the trap are not being captured but leave the ion trap through the rear electrode and would reach the channeltron detector, thereby reducing its life-time. Therefore, during ion accumulation, the channeltron is protected by a positive voltage (200 V) applied to the detector lens positioned between the rear end cap electrode and the channeltron. During ion analysis this voltage is switched back to 0 V. This mode of gating, for the ion source and the detector, is similar to the method used by Orient and Chutjian [31].

The timing and the voltages of the National Instruments boards are controlled by a Labview program (National Instruments, USA) that also displays and records the data. The program is also used for mass calibration and allows calculating the waveforms needed for Filtered Noise Fields, CID and mass range extension.

3. Experimental results

A typical mass spectrum for residual gas recorded with the IT-AMS is shown in Fig. 4. The signals that have been used to create the stick spectrum consist of 52 data points that are summed to obtain the unit mass value. The spectrum was recorded when the inlet of the IT-AMS was closed, so the signals at $m/z > 40$ result mainly from evaporating organic components inside the vacuum system. Therefore, these signals are relatively constant and have no large effect on the sensitivity. When the inlet of the IT-AMS is opened and an aerosol filter is used the intensities of these peaks change only very little because the aerodynamic lens has a high transmission for particles but not for the gas phase. Ions were accumulated for 10 ms followed by a reaction time of 100 ms when no ions were allowed to enter the trap and the amplitude at the ring electrode was kept constant. It was found that the application of this additional reaction time improves the signal-to-noise ratio and also improves mass resolving power slightly. This is probably due to the fact that the ions need an additional cooling time to finally collapse into the trap center at the relatively low helium pressure of 1.0×10^{-4} hPa [32]. The time for the mass scan from m/z 15 to m/z 126 was 61 ms, which corresponds to a scan rate of approximately 1800 amu/s. The spectrum displays an average of 100 single spectra recorded within less than 20 s. From comparison of the highest and lowest ion rates the dynamic range is found to be four to five orders of magnitude. Ions at m/z 23 (Na^+) and m/z 39 ($^{39}K^+$) are emitted by the vaporizer; their intensities vary depending on vaporizer temperature and its age. Strong signals are also observed at m/z 19 (H_3O^+), m/z 30 (NO^+) and m/z 32 (O_2^+), whereas only comparatively small peaks are observed at m/z 14 (N^+), m/z 16 (O^+), m/z 18 (H_2O^+) and m/z 28 (N_2^+) due to reactions that include charge exchange and proton transfer [16,33]. If no reaction time is applied these ions can also be observed at higher intensities.

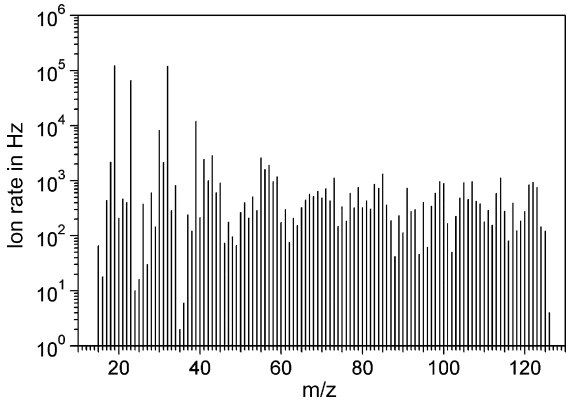

Fig. 4. Typical mass spectrum from the residual gas phase averaged over 100 single spectra.

Table 1
Calculated duty-cycles for two different cases for the IT-AMS

	High resolution case	High sensitivity case
Empty time in ms	10	10
Ion accumulation time in ms	10	200
Reaction time in ms	100	0
Mass scan time in ms	60	60
Total cycle time in ms	180	270
Trapping efficiency in percentage	1–5	1–5
Duty-cycle in percentage	0.03–0.14	0.37–1.85

The spectra shown in Fig. 4 and the applied timing intervals for the sampling and the reaction represent a case when the settings of the IT-AMS are selected in a way to maximize the signal-to-noise ratio and the mass resolving power. In this case the duty-cycle is rather low because of the small fraction of time spent for ion accumulation in relation to the total cycle time. The duty-cycle 'dc' for a single m/z can be calculated according to the expression:

$$\mathrm{dc} = \frac{t_a}{t_e + t_a + t_r + t_s} \times \mathrm{TE} \times 0.5 \quad (4)$$

where t_e is the time spent for emptying the trap, t_a the ion accumulation time, t_r the reaction time, t_s the time for the mass scan and TE is the trapping efficiency. The factor 0.5 is used here to take into account the time that is spent for background measurements when no particles are analyzed. The duty-cycle depends strongly on the applied accumulation time and whether a reaction time is applied or not. Table 1 gives typical values for a high resolution case and a high sensitivity case. It can be seen that a duty-cycle of almost 2% can be reached if a maximum trapping efficiency of 5% is assumed. In this case the duty-cycle exceeds the value of 0.03% for the Q-AMS but is lower than the maximum value of 22.5% for the ToF-AMS [19]. The settings for the high sensitivity mode given in Table 1 were used to determine the detection limits of nitrate and sulfate (see below).

Fig. 5 shows the ion signals from residual gas at m/z 41–43. In contrast to the spectrum shown in Fig. 4 this spectrum was recorded at a reduced scan rate of 223 amu/s and axial modulation was applied to achieve resonant ion ejection at $q_z = 0.876$ instead of the generally used ejection at $q_z = 0.908$. Both, the reduced scan rate and the resonant excitation are known to increase mass resolving power [34,35]. The inset of Fig. 5 shows the signal at m/z 43 and different Lorentzian fit curves. It can be clearly seen that the signal consists of two peaks which arise most probably from $C_2H_3O^+$ (m/z 43.0184) and from $C_3H_7^+$ (m/z 43.0548). The fit curve for the larger peak reveals a mass resolving power (FWHM) slightly higher than 1500 which is high enough to separate $C_2H_3O^+$ from $C_3H_7^+$. So far, the high-resolution time-of-flight aerosol mass spectrometer (HR-ToF-AMS) was the only aerosol mass spectrometer using the Aerodyne inlet and evaporation/ionization system capable to separate different organic ions at the same nominal m/z [19]. In the future, we expect to increase the mass resolving power for the IT-AMS even further by trying different ejection frequencies and reducing scan rate further which is currently limited by the

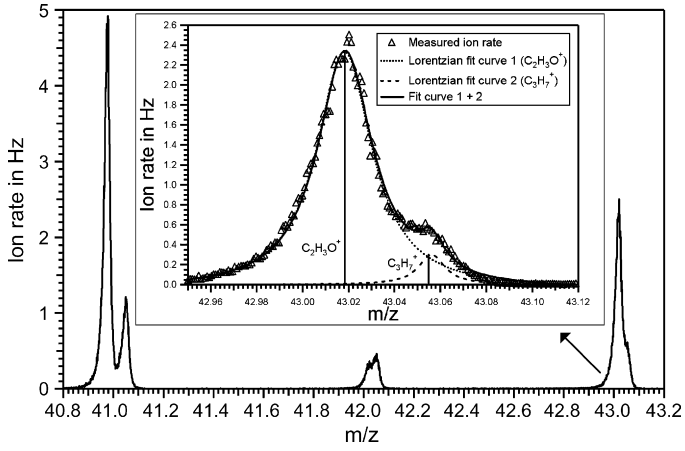

Fig. 5. Residual gas mass spectrum recorded at a reduced scan rate of 223 amu/s and an axial modulation frequency of 540 kHz ($q_z = 0.876$). Mass resolving power (at FWHM) determined by the Lorentzian fit curve 1 has a value of 1542.

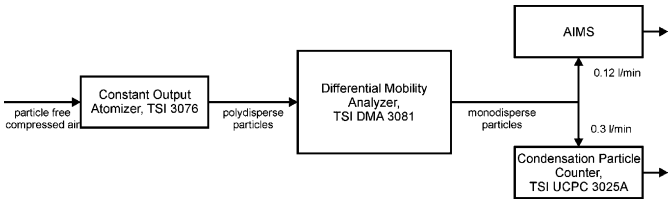

Fig. 6. Experimental set-up for mass calibration measurements with the IT-AMS. From particle density, size and number concentration the aerosol mass concentration can be calculated and compared to ion rates measured with the IT-AMS for *m/z* values that can be attributed to the particles.

electronics. A drastic enhancement is also expected from phase-locking the drive frequency to the resonant excitation frequency as shown by Londry and March [36]. This will allow the ejection of ions at well-defined times in each cycle and will therefore lead to a reduced spread of the peak positions when many spectra are averaged. By applying this method to a three-dimensional ion trap values greater than 50,000 have been achieved [36]. In future, we also want to phase-lock the two frequencies in the IT-AMS. However, even when no axial modulation is used and a higher scan rate of 1800 amu/s is applied (as it was used for recording the spectrum in Fig. 4) mass resolution is quite high. In this case a value of 480 is found for *m/z* 43. But it should also be noted that the mass resolving power is mass dependent. When the fast scan rate is used a value of 370 was found for *m/z* 32 and a value of 800 for *m/z* 121.

The IT-AMS measures the chemical composition of the non-refractory component of aerosol particles quantitatively. Nevertheless, it is difficult to calculate the mass concentration of a certain aerosol species directly from the measured ion rates at the *m/z* values that can be attributed to that aerosol species as it can be done for the Q-AMS data [37,38]. Although the AMS and the IT-AMS use an identical electron impact ion source, which allows quantitative measurements, there is a substantial difference in the mass analysis. The transmission efficiency of the mass spectrometer which has to be known for the calculation is different. The transmission coefficient for the linear quadrupole is generally assumed to be unity for all *m/z* values that can be analyzed [37]. The transmission efficiency of the IT-AMS depends on two factors: First, the efficiency for focusing all ions into the trap through the small hole in the front end cap electrode and second, the efficiency for capturing the incoming ions. This efficiency has been calculated and measured to be approximately 1–5% (depending on the mean free path of the ions) under optimum conditions for externally generated ions from a continuous ion source [39]. While the first factor is constant for all *m/z* values, the second factor is mass dependent (see, e.g., ref. [40]). The trapping efficiency can be estimated by experimental or theoretical studies and therefore a direct quantification of the measured signals is feasible. This issue will be addressed in a forthcoming publication in detail. Here we use the first approach for quantitative measurements to determine calibration curves for some important atmospheric aerosol components. The set-up for these measurements is shown in Fig. 6. For these experiments, standard instruments were used to produce and to classify aerosol particles. A detailed description of these methods is given in the instrument manuals or in textbooks [41,42]. Liquid or solid material that will be analyzed is dissolved in water and atomized with pressurized particle-free air in a Constant Output Atomizer (Model 3076, TSI Inc., USA). The polydisperse aerosol is dried in a diffusion section and then classified with a Differential Mobility Analyzer (DMA, Model 3081, TSI Inc.). The DMA uses a bipolar charger (^{85}Kr) and classifies the particles according to their electrical mobility. By adjusting a fixed voltage, particles with a certain electrical mobility can be selected. It should be noted here that multiply charged particles have to be excluded in the measurements. These particles are larger than the selected particle size but have the same electrical mobility and would therefore also reach the IT-AMS. Even at low concentrations they could contribute substantially to the total aerosol mass concentration. Therefore, an impactor was used in front of the DMA. Since the available impactor could only remove relatively large particles (d_{50} cut size ~400 nm for the impactor geometry and the chosen flow rate) all measurements were carried out with $d = 300$ nm (electrical mobility diameter) particles. Finally, the particle number concentration is measured in parallel to the recorded mass spectra with an Ultrafine Condensation Particle Counter (UCPC 3025A, TSI Inc.). From the known density, the selected diameter and the measured concentration the aerosol mass concentration can be calculated.

Fig. 7 shows a mass calibration curve for nitrate from ammonium nitrate particles (NH_4NO_3). As an indicator for nitrate the ion rate at *m/z* 46 (NO_2^+) is used. The error bars for the ion rate result from the standard deviation over several measurements. The line fit through the data points with the intercept fixed to zero indicates an excellent correlation between the measured signal and the nitrate mass concentration for values between 0.65 and 14.14 μg/m^3 nitrate. Note that the ion rate measured with the IT-AMS is considerably lower than the rate measured with the AMS for the same aerosol mass concentrations because of the lower ion transmission within the IT-AMS (see discussion above). A calibration curve has also been recorded for sulfate (not shown) from the signal at *m/z* 48 (SO^+) that shows a good linear correlation as well for concentrations between 1.00 and

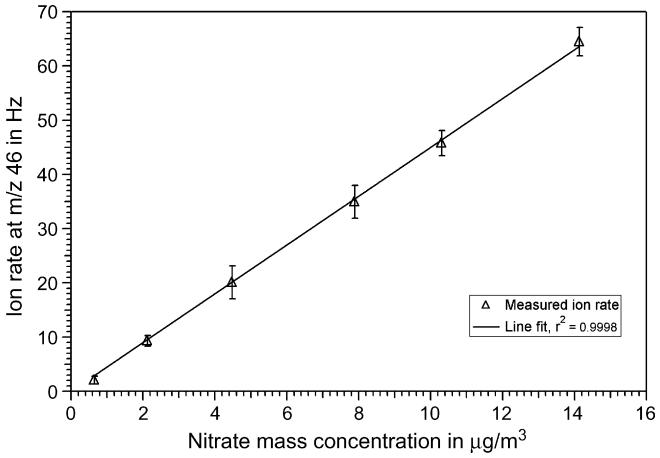

Fig. 7. Ion rate at m/z 46 (NO_2^+) as a function of different nitrate mass concentrations. For these measurements different number concentrations of monodisperse ammonium nitrate (NH_4NO_3) particles have been generated and measured with the set-up shown in Fig. 6.

17.61 µg/m^3 sulfate. The concentrations that have been measured here include typical average atmospheric concentrations of these species (see, e.g., refs. [43–45]). Calibrations should be repeated from time to time because trap electrodes get dirty sometimes, especially after measurements at high aerosol loads. This experience was made after measurements in the laboratory were carried out at concentrations larger than 1 mg/m^3 over several hours. Whether the same effect can occur under atmospheric concentrations and longer time scales has not been observed up to now. Additionally, the efficiency of the detector decreases with time and therefore has to be monitored in a similar way as for the Q- and the ToF-AMS (see, e.g., ref. [46]). Since the number of air molecules entering the instrument is constant for ground-based measurements, the detector efficiency can be monitored by tracking the intensity of an air ion peak. Although the intensity of some of these peaks is influenced by reactions (e.g., m/z 28; see Fig. 4) this procedure can be applied when the timing sequence that is used for the measurements is identical to the one used during the calibration. Detection limits for different aerosol components have been determined for the IT-AMS. The detection limit is the aerosol mass concentration which creates a signal that is on average larger than $\mu_B + 3\sigma_B$, where μ_B and σ_B are the average and the standard deviation of a particle-free background measurement, respectively. The detection limits found for an averaging time of 1 min are 0.16 µg/m^3 for nitrate and 0.65 µg/m^3 for sulfate.

These values are currently about a factor of 10 higher for nitrate and a factor of 25 for sulfate, when compared to the detection limits found for the Q-AMS by Hings [47]. DeCarlo et al. [19] also determined the detection limits for the Q-AMS and found somewhat higher values than Hings. When compared to these values the factors are 5 and 4 for nitrate and sulfate, respectively. It is noteworthy here that for the calculation of the mass concentration values it has been assumed that the particles that leave the DMA are spherical and that the geometric diameter equals the electrical mobility diameter. If the particles are shaped irregularly then the electrical mobility diameter will always be larger than the volume equivalent diameter [48] and the calculated particle mass will therefore be overestimated. This means that the detection limits for the IT-AMS given above are a conservative estimate and might be somewhat lower since it seems likely that at least ammonium nitrate particles are non-spherical [17].

However, the determined detection limits are lower than atmospheric concentrations in many cases and it is planned to reduce detection limits in the future. This can probably be done by improving the control of the filament emission current. This is crucial because fluctuations of the emission current directly translate into fluctuations of the measured background ions and thereby influence the detection limits. Precise control of the emission current is difficult for the IT-AMS due to the inevitable gating of the ion source voltage.

From the measured ion rate at m/z 46 the ionization efficiency for NO_2^+ can be estimated. The ionization efficiency is defined as the sum of all ions produced from a specific species divided by the number of molecules from that species. However, even if different ions are being produced, the ionization efficiency can be related to a single m/z value. To calculate the ionization efficiency for m/z 46 from nitrate the measured ion rate needs to be corrected first. The ion transmission to the trap, the trapping efficiency and the detector efficiency have been taken into account. These values have been assumed to be 0.5, 0.01 and 0.80 for the IT-AMS, respectively. With the equation given by Jimenez et al. [37] an ionization efficiency for NO_2^+ from particulate nitrate can be estimated to be 1×10^{-7}. This value is lower than the approximate value of 1×10^{-6} given by Canagaratna et al. [6] for nitrate for the AMS. However, the difference is probably due to the fact that the latter value relates to the combined ion rate of NO^+ and NO_2^+ and not just to NO_2^+ as it is the case in this study. In addition, the operation of the IT-AMS is currently limited to the use of a relatively low emission current of only 100 µA due to the electronics. The IT-AMS has also been inter-compared with the Q-AMS. Fig. 8 shows a comparison between the two instruments for measured aerosol nitrate mass concentrations in urban air in Mainz, Germany. The time resolution was adjusted to 10 min. The aerosol nitrate concentrations for the IT-AMS

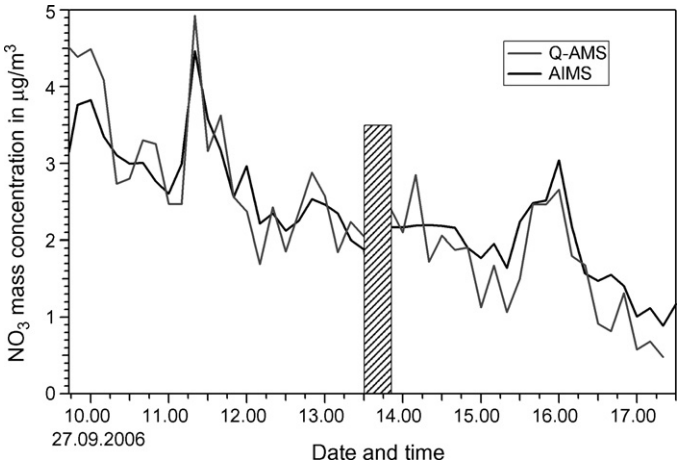

Fig. 8. Comparison between the IT-AMS and the Q-AMS for nitrate mass concentrations found in urban air.

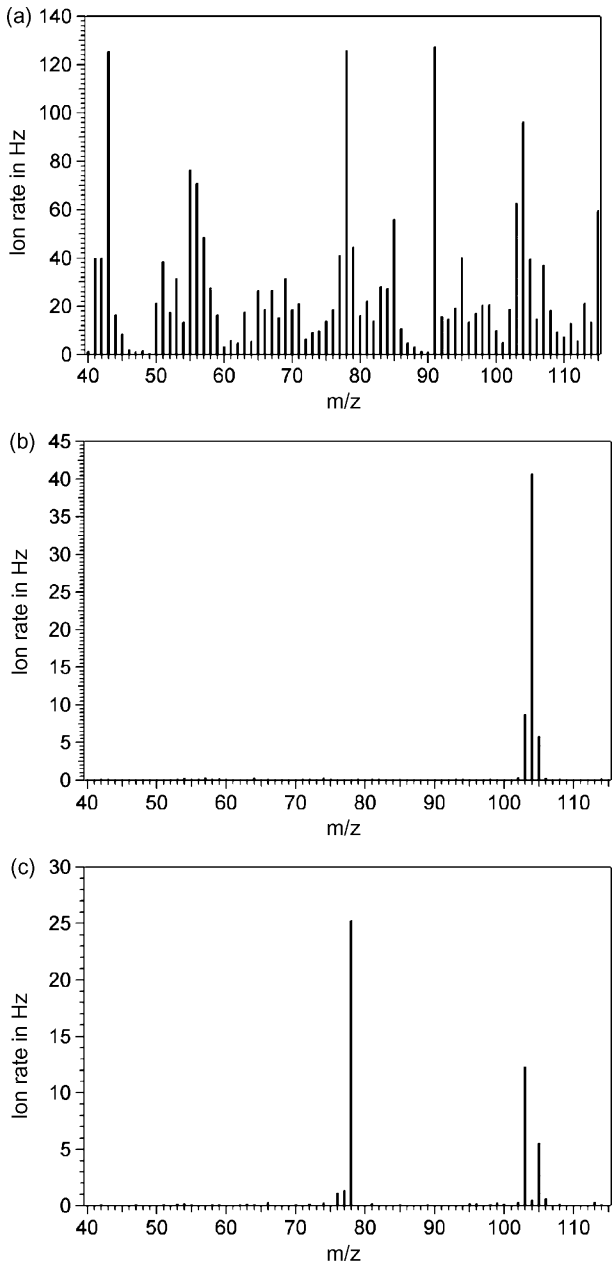

Fig. 9. A sequence of a MS/MS-study performed for ions from polystyrene latex aerosol particles. In (a) the raw mass spectrum is shown. In (b) the ions of the monomer at *m/z* 104 ($C_8H_8^+$) have been isolated by Filtered Noise Fields. Resonant excitation with a peak voltage of 80 mV has been applied for a period of 100 ms resulting in fragmentation mainly to *m/z* 78 ($C_6H_6^+$) (c).

have been calculated from a calibration curve similar to the one shown in Fig. 7. Overall, the concentrations measured by the two instruments indicate good agreement.

Fig. 9 shows a MS/MS-study. In Fig. 9a, the raw mass spectrum of ions from polystyrene latex spheres (PSLs $(C_8H_8)_n$) including the background residual gas spectrum is shown. The aerosol mass concentration derived from the measured number concentration of the monodisperse particles is ~8 μg/m^3. In the spectrum a distinct peak occurs at *m/z* 104 from ions of the monomer ($C_8H_8^+$). In Fig. 9b, these ions are isolated by Filtered Noise Fields. The neighboring peaks are still abundant, but their intensities have decreased substantially relative to the *m/z* 104 signal. In Fig. 9c, the monomer ions have been excited resonantly which results in energetic collisions with helium atoms and induces fragmentation. For the excitation a sine wave was applied to the end-cap electrodes to excite only *m/z* 104 ions. An excitation time of 100 ms has been used with an amplitude of 80 mV (zero to peak). While the signal at *m/z* 104 has vanished almost completely in (c) a peak at *m/z* 78 occurs due to loss of the neutral C_2H_2 from the monomer ions. CID efficiency can be estimated from this example to be greater than 60%. The overall efficiency, which includes the isolation of the monomer ions, is approximately 25%. Since the excitation is carried out at a sine wave that contains only a single frequency and therefore only affects a single integer *m/z* the ejection of the direct neighbors is not absolutely necessary prior to the CID which means that even a higher efficiency can be reached. The complete isolation is only necessary if the peak at M-1 was a significant daughter ion. During trapping of the ions the q_z-value for *m/z* 104 was 0.09. By changing the voltage at the ring electrode during CID this value was changed to 0.34 thereby increasing the potential well depths in the trap center (see ref. [27]) for all ions which allows to transfer more energy to the ions for fragmentation without these ions being lost [49].

4. Summary and outlook

A novel Ion Trap Aerosol Mass Spectrometer has been developed and characterized. The instrument consists of the combination of an in-house designed and machined three-dimensional quadrupole ion trap mass analyzer and an inlet chamber with an aerodynamic lens, a particle vaporizer and an ion source identical to the Aerodyne Aerosol Mass Spectrometer.

The IT-AMS allows quantitative measurements of the non-refractory fraction of atmospheric aerosol particles as demonstrated by calibrations with laboratory-generated monodisperse particles. The recorded calibration curves show an excellent linear correlation between ion signal and generated aerosol mass concentration. The overall detection limits (1 min averages) were found to be 0.16 μg/m^3 for nitrate and 0.65 μg/m^3 for sulfate. A comparison with the commercial Q-AMS for urban particulate nitrate concentrations between ~0.5 and 5 μg/m^3 shows the applicability of the IT-AMS for ambient aerosol measurements. The capability of performing MS/MS-studies is unique among the aerosol mass spectrometers using the Aerodyne inlet and it was demonstrated that the CID efficiency is larger than 60% for ions from polystyrene latex particles. Although the mass concentration used for this experiment was relatively high (~8 μg/m^3), the good signal-to-noise ratio achieved during the measurements indicates that MS/MS-experiment can be performed also at much lower aerosol concentrations. However, since the ambient aerosol contains numerous different organic substances with typical concentrations in the ng/m^3 range [50], the sensitivity of the IT-AMS needs to be increased further to enable the study of the chemical composition of such particles. Nevertheless, with the current sensitivity it will already be possible to study exhaust from diesel trucks or biomass burning and to carry out smog chamber

experiments to study the formation of secondary aerosol. The maximum mass resolving power has been determined to be larger than 1500. This value is high enough to allow the differentiation between $C_2H_3O^+$ and $C_3H_7^+$ at m/z 43.

In the future it is planned to calculate aerosol mass concentrations directly from the measured ion rates, without the necessity of recording calibration curves for each individual ion species. This can be done by theoretical calculations of the trapping efficiencies for the most important ions if the ionization efficiency is known or if it can be estimated. Improving the detection limits is necessary to allow measurements in remote regions where aerosol mass concentrations are low. The installation of a VUV lamp for single photon ionization is planned for soft ionization alternatively to electron impact ionization [51–53]. Together with the large mass range that is accessible with the IT-AMS and the MS/MS-capability we expect that this allows the speciation of unknown organic aerosol compounds. The expected lower ionization efficiency of single photon ionization compared to electron impact ionization could probably be compensated, at least partly, by the fact that the gating of the ion current to the trap will become easier and will probably reduce noise. The installation of two chopper wheels is planned for recording size-resolved particle spectra.

Acknowledgements

We thank Thomas Böttger and Michael Flanz for mechanical and electronic engineering support. We thank Johannes Schneider for providing the Q-AMS inter-comparison. Helpful discussions with John Jayne and Doug Worsnop from Aerodyne Inc. are acknowledged. Valuable comments from two anonymous referees are acknowledged. Financial support from the Max Planck Society, the Johannes Gutenberg University and the German Research Foundation (Interdisciplinary Research Training Group Program 826 on "Trace analysis of elemental species: Development of methods and applications") is gratefully acknowledged.

References

[1] R.C. Sullivan, K.A. Prather, Anal. Chem. 77 (2005) 3861.
[2] S. Fuzzi, M.O. Andreae, B.J. Huebert, M. Kulmala, T.C. Bond, M. Boy, S.J. Doherty, A. Guenther, M. Kanakidou, K. Kawamura, V.-M. Kerminen, U. Lohmann, L.M. Russell, U. Pöschl, Atmos. Chem. Phys. 6 (2006) 2017.
[3] M. Kanakidou, J.H. Seinfeld, S.N. Pandis, I. Barnes, F.J. Dentener, M.C. Facchini, R. Van Dingenen, B. Ervens, A. Nenes, C.J. Nielsen, E. Swietlicki, J.P. Putaud, Y. Balkanski, S. Fuzzi, J. Horth, G.K. Moortgat, R. Winterhalter, C.E.L. Myhre, K. Tsigaridis, E. Vignati, E.G. Stephanou, J. Wilson, Atmos. Chem. Phys. 5 (2004) 1053.
[4] C.A. Noble, K.A. Prather, Mass Spectrom. Rev. 19 (2000) 248.
[5] D.G. Nash, T. Baer, M.V. Johnston, Int. J. Mass Spectrom. 258 (2006) 2.
[6] M.R. Canagaratna, J.T. Jayne, J.L. Jimenez, J.D. Allan, M.R. Alfarra, Q. Zhang, T.B. Onasch, F. Drewnick, H. Coe, A. Middlebrook, A. Delia, L.R. Williams, A.M. Trimborn, M.J. Northway, P.F. DeCarlo, C.E. Kolb, P. Davidovits, D.R. Worsnop, Mass Spectrom. Rev. 26 (2007) 185.
[7] R.A. Gieray, P.T.A. Reilly, M. Yang, W.B. Whitten, J.M. Ramsey, J. Microbiol. Methods 29 (1997) 191.
[8] P.T.A. Reilly, R.A. Gieray, W.B. Whitten, J.M. Ramsey, Env. Sci. Technol. 32 (1998) 2672.
[9] R.A. Gieray, P.T.A. Reilly, M. Yang, W.B. Whitten, J.M. Ramsey, Anal. Chem. 70 (1998) 117.
[10] W.A. Harris, P.T.A. Reilly, W.B. Whitten, J.M. Ramsey, Rev. Sci. Instrum. 76 (2005) 064102.
[11] W.A. Harris, P.T.A. Reilly, W.B. Whitten, Int. J. Mass Spectrom. 258 (2006) 113.
[12] W.A. Harris, P.T.A. Reilly, W.B. Whitten, Anal. Chem. 79 (2007) 2354.
[13] S. Wang, C.A. Zordan, M.V. Johnston, Anal. Chem. 78 (2006) 1750.
[14] S. Wang, M.V. Johnston, Int. J. Mass Spectrom. 258 (2006) 50.
[15] T. Hoffmann, R. Bandur, U. Marggraf, M. Linscheid, J. Geophys. Res. 103 (D19) (1998) 25569.
[16] C.N. Dalton, M. Jaoui, R.M. Kamens, G.L. Glish, Anal. Chem. 77 (2005) 3156.
[17] J.T. Jayne, D.C. Leard, X. Zhang, P. Davidovits, K.A. Smith, C.E. Kolb, D.R. Worsnop, Aerosol Sci. Technol. 33 (2000) 49.
[18] F. Drewnick, S.S. Hings, P. DeCarlo, J.T. Jayne, M. Gonin, K. Fuhrer, S. Weimer, J.L. Jimenez, K.L. Demerjian, S. Borrmann, D.R. Worsnop, Aerosol Sci. Technol. 39 (2005) 637.
[19] P.F. DeCarlo, J.R. Kimmel, A. Trimborn, M.J. Northway, J.T. Jayne, A.C. Aiken, M. Gonin, K. Fuhrer, T. Horvath, K.S. Docherty, D.R. Worsnop, J.L. Jimenez, Anal. Chem. 78 (2006) 8281.
[20] X. Zhang, K.A. Smith, D.R. Worsnop, J. Jimenez, J.T. Jayne, C.E. Kolb, Aerosol Sci. Technol. 36 (2002) 617.
[21] X. Zhang, K.A. Smith, D.R. Worsnop, J.L. Jimenez, J.T. Jayne, C.E. Kolb, J. Morris, P. Davidovits, Aerosol Sci. Technol. 38 (2004) 619.
[22] J.A. Huffman, J.T. Jayne, F. Drewnick, A.C. Aiken, T. Onasch, D.R. Worsnop, J.L. Jimenez, Aerosol Sci. Technol. 39 (2005) 1143.
[23] J. Franzen, R.-H. Gabling, M. Schubert, Y. Wang, in: R.E. March, J.F.J. Todd (Eds.), Practical Aspects of Ion Trap Mass Spectrometry/Fundamentals of Ion Trap Mass Spectrometry, vol. 1, CRC Press Inc., 1995, p. 49.
[24] J. Curtius, K.D. Froyd, E.R. Lovejoy, J. Phys. Chem. A 105 (2001) 10867.
[25] G.C. Stafford Jr., P.E. Kelley, J.E.P. Syka, W.E. Reynolds, J.F.J. Todd, Int. J. Mass Spectrom. Ion Proc. 60 (1984) 85.
[26] D.A. Dahl, Int. J. Mass Spectrom. 200 (2000) 3.
[27] R.E. March, J. Mass Spectrom. 32 (1997) 351.
[28] R.E. Kaiser Jr., R.G. Cooks, G.C. Stafford Jr., J.E.P. Syka, P.H. Hemberger, Int. J. Mass Spectrom. Ion Proc. 106 (1991) 79.
[29] L. Chen, T.-C.L. Wang, T.L. Ricca, A.G. Marshall, Anal. Chem. 59 (1987) 449.
[30] M.H. Soni, R.G. Cooks, Anal. Chem. 66 (1994) 2488.
[31] O.J. Orient, A. Chutjian, Rev. Sci. Instrum. 73 (2002) 2157.
[32] H.-F. Wu, J.S. Brodbelt, Int. J. Mass Spectrom. Ion Proc. 115 (1992) 67.
[33] A.K. Ottens, C.R. Arkin, T.P. Griffin, P.T. Palmer, W.W. Harrison, Int. J. Mass Spectrom. 243 (2005) 31.
[34] D.E. Goeringer, W.B. Whitten, J.M. Ramsey, S.A. McLuckey, G.L. Glish, Anal. Chem. 64 (1992) 1434.
[35] F.A. Londry, G.J. Wells, R.E. March, Rapid Commun. Mass Spectrom. 7 (1993) 43.
[36] F.A. Londry, R.E. March, Int. J. Mass Spectrom. Ion Proc. 144 (1995) 87.
[37] J.L. Jimenez, J.T. Jayne, Q. Shi, C.E. Kolb, D.R. Worsnop, I. Yourshaw, J.H. Seinfeld, R.C. Flagan, X. Zhang, K.A. Smith, J.W. Morris, P. Davidovits, J. Geophys. Res. 108 (D7) (2003) 8425, doi:10.1029/2001JD001213.
[38] M.R. Alfarra, H. Coe, J.D. Allan, K.N. Bower, H. Boudries, M.R. Canagaratna, J.L. Jimenez, J.T. Jayne, A.A. Garforth, S.-M. Li, D.R. Worsnop, Atmos. Env. 38 (2004) 5745.
[39] A.D. Appelhans, D.A. Dahl, Int. J. Mass Spectrom. 216 (2002) 269.
[40] K. Yoshinari, Rapid Commun. Mass Spectrom. 14 (2000) 215.
[41] W.C. Hinds, Aerosol Technology: Properties, Behavior, and Measurement of Airborne Particles, second ed., John Wiley & Sons Inc., New York, 1999.
[42] P.A. Baron, K. Willeke, Aerosol Measurement. Principles, Techniques and Applications, second ed., John Wiley & Sons Inc., New York, 2001.
[43] D. Topping, H. Coe, G. McFiggans, R. Burgess, J. Allan, M.R. Alfarra, K. Bower, T.W. Choularton, S. Decesari, M.C. Facchini, Atmos. Env. 38 (2004) 2111.
[44] D. Salcedo, T.B. Onasch, K. Dzepina, M.R. Canagaratna, Q. Zhang, J.A. Huffman, P.F. DeCarlo, J.T. Jayne, P. Mortimer, D.R. Worsnop, C.E. Kolb, K.S. Johnson, B. Zuberi, L.C. Marr, R. Volkamer, L.T. Molina, M.J. Molina,

B. Cardenas, R.M. Bernabé, C. Márquez, J.S. Gaffney, N.A. Marley, A. Laskin, V. Shutthanandan, Y. Xie, W. Brune, R. Lesher, T. Shirley, J.L. Jimenez, Atmos. Chem. Phys. 6 (2006) 925.
[45] J. Schneider, S.S. Hings, B.N. Hock, S. Weimer, S. Borrmann, M. Fiebig, A. Petzold, R. Busen, B. Kärcher, J. Aerosol Sci. 37 (2006) 839.
[46] J.D. Allan, J.L. Jimenez, P.I. Williams, M.R. Alfarra, K.N. Bower, J.T. Jayne, H. Coe, D.R. Worsnop, J. Geophys. Res. 108 (D3) (2003) 4090, doi:10.1029/2002JD002358.
[47] S.S. Hings, PhD thesis, Johannes Gutenberg University, Mainz, 2007.
[48] P.F. DeCarlo, J.G. Slowik, D.R. Worsnop, P. Davidovits, J.L. Jimenez, Aerosol Sci. Technol. 38 (2004) 1185.
[49] J.V. Johnson, R.E. Pedder, R.A. Yost, Int. J. Mass Spectrom. Ion Proc. 106 (1991) 197.
[50] J.J. Schauer, W.F. Rogge, L.M. Hildemann, M.A. Mazurek, G.R. Cass, Atmos. Env. 30 (22) (1996) 3837.
[51] F. Mühlberger, T. Streibel, J. Wieser, A. Ulrich, R. Zimmermann, Anal. Chem. 77 (2005) 7408.
[52] R. Zimmermann, Anal. Bioanal. Chem. 381 (2006) 57.
[53] M.J. Northway, J.T. Jayne, D.W. Toohey, M.R. Canagaratna, A. Trimborn, K.-I. Akiyama, A. Shimono, J.L. Jimenez, P.F. DeCarlo, K.R. Wilson, D.R. Worsnop, Aerosol Sci. Technol., in press.